

ROTOR TRIM BY A NEURAL MODEL-PREDICTIVE AUTO-PILOT

C.L. Bottasso and L. Riviello

Dipartimento di Ingegneria Aerospaziale, Politecnico di Milano, Milano, Italy

Abstract

Modern comprehensive finite element-based tools for the aeromechanic analysis of rotorcraft require the ability of accurately computing the model trim settings. Proportional control laws (auto-pilots) have often been used in many practical instances, because this technique is not directly related to the complexity of the system. On the other hand, classical auto-pilots must be carefully tuned for every desired flight condition. This work focuses on improving the auto-pilot technique by means of non-linear model-predictive control. A reference model of the system augmented with an adaptive neural element is used to predict the system response and solve an optimal control problem, which in turn produces the control strategy that is used for regulating the system. The adaptive element allows for the identification and correction of the mismatch between reduced model and controlled system, thereby improving the predictive capabilities of the controller. Tests on the wind-tunnel trim of a rotor multibody model and comparisons with an existing implementation of a classical auto-pilot are discussed.

List of Symbols

| | | | |
|----------------------------|--|-------------------|--|
| $\tilde{(\bullet)}$ | system (comprehensive model) quantity | p | reduced model parameters |
| $(\bullet)^{\text{reg}}$ | model predictive regulation problem quantity | $(\dot{\bullet})$ | derivative with respect to time |
| $(\bullet)^{\text{steer}}$ | steering problem quantity | t | time |
| $(\bullet)^{\text{adapt}}$ | model adaption problem quantity | T_i | initial time |
| $(\bullet)^*$ | given or desired value | T_f | final time |
| \tilde{x} | system states | J | cost function |
| $\tilde{\lambda}$ | system Lagrange multipliers | T | rotor revolution period |
| \tilde{u} | system controls | μ | rotor advance ratio (far field velocity / rotor tip velocity) |
| \tilde{y} | system outputs | | |
| y | reduced model states | | |
| u | reduced model controls | | |

Introduction

The word "trim" is part of the large vocabulary shared by the naval and aeronautical communities, and indicates the control settings, attitude and cargo disposition required to obtain

a desired steady condition for a sailing or flying vehicle. In most cases, as for fixed wing aircrafts, boats or even cars and motorcycles, steady condition simply means that control inputs are held fixed and the components of the vehicle linear and angular velocities are constant in a body attached frame. A rotorcraft, however, flies by means of rotating aerodynamic surfaces, so it is always excited by harmonic loads. Therefore, the vehicle can be controlled so as to follow a particular periodic orbit, with constant controls and harmonic system response. This trimmed flight condition is characterized by having constant values of the average over a rotor revolution of the body components of the linear and angular velocities. Computing such a flight condition is a much more difficult task than in the case of a fixed wing aircraft.

As for any other vehicle, the determination of the trim settings plays a central role in the analysis of the dynamic characteristics and stability of a rotorcraft. In fact, to analyze the aeroelastic stability, handling qualities and vibratory levels, the system is commonly perturbed about the periodic orbit corresponding to the trim condition. The resulting set of perturbation equations strongly depends upon the reference solution about which the perturbation takes place. Hence, the trim solution has to be computed with sufficient accuracy. Unfortunately, for numerical models the trim settings can not be estimated using experimental data, because of the unavoidable approximations that are introduced every time a virtual prototype of the real system is created. For example, measured controls obtained by flight test data cannot trim a numerical rotorcraft model, which would simply drift away from the desired periodic solution, or even diverge in free-flight cases.

Nowadays, comprehensive finite element-based analysis tools [2, 14] are used to model rotary wing vehicles with a high level of detail. Such tools implement mathematical models of the elastic blades, control linkages, drive train, fuselage, actuators, hydraulic systems, engines, sensors, etc. Rotorcraft codes can be coupled with different time-accurate aero-

dynamic models, like dynamic inflow [13], free-wake models [4], but also computational fluid dynamics modules to account for several complex features of the flow. Hence, modern rotorcraft aeroelastic analyses require the ability to solve multi-field, highly non-linear problems, characterized by a large number of degrees of freedom. This research focuses on the efficient trim of such models.

The specialized literature reports a few strategies for the trim of rotorcraft models, which have been developed and applied over the last thirty years. These strategies include the harmonic balance, periodic shooting, finite elements in time, quasi-Newton and the auto-pilot methods. Some of these methods require the solution of the complete set of trim equations for the system, so the resulting computational effort is proportional to the complexity of the model. In the auto-pilot approach, the system is augmented with a control law that steers the system towards the desired trim condition, regardless of the number of degrees of freedom of the rotorcraft numerical model. On the other hand, controls are in this case promoted to time-varying quantities with their own dynamic behavior, so limit cycles can often affect the solution and the desired steady-state condition is not reached. Moreover, feedback is generally provided through the use of appropriate gains on the error on the trim constraints, i.e. on the desired values of average states and/or loads. Therefore, it is often difficult to tune the values of the gains in order to achieve both stability and a satisfactory performance of the controller. Reference [12] analyzes the rotorcraft trim problem in detail and provides an ample bibliography on this topic.

In this research, a new auto-pilot based on a neural-adaptive non-linear model-predictive (NMP) control is introduced. We believe that this approach has the potential for sharing all of the positive features of a classical auto-pilot, while avoiding its drawbacks. In particular, some classical results on the theory of NMP control and neural networks can be used to infer the stability of the controller in a non-linear setting (a topic that is not addressed in this paper for space limitations) and the avoidance of

limit cycle oscillations in the solution. Moreover, the use of a non-linear reduced model to predict the system behavior translates into superior performance of the new approach, which preserves at the same time affordable computational costs and the applicability to comprehensive models of arbitrary complexity.

Rotorcraft Trim Formulation

The governing equations for a virtual prototype $\tilde{\mathcal{M}}$ of a rotorcraft can be written in a “multibody fashion” as

$$\tilde{\mathbf{f}}(\dot{\tilde{\mathbf{x}}}, \tilde{\mathbf{x}}, \tilde{\boldsymbol{\lambda}}, \tilde{\mathbf{u}}) = 0, \quad (1a)$$

$$\tilde{\mathbf{c}}(\tilde{\mathbf{x}}, \tilde{\mathbf{x}}) = 0. \quad (1b)$$

The first set of equations, (1a), represents the equations of dynamic equilibrium and the kinematic equations, and the second set, (1b), represents possible holonomic and non-holonomic constraint conditions. The vector $\tilde{\mathbf{x}}$ denotes the system states, $\tilde{\boldsymbol{\lambda}}$ are the Lagrange multipliers which enforce the constraints (1b), and $\tilde{\mathbf{u}}$ are the controls.

The states $\tilde{\mathbf{x}}$ may include displacements, rotations, linear and angular velocities, and possible internal states describing the dynamics of mechanical components such as engines, actuators and sensors. When flexible structural elements are present in the model, the states will also include degrees of freedom associated with the spatial discretization or modal amplitudes. Furthermore, the aerodynamic module can be provided by coupling with external codes or by a suitable set of equations and associated aerodynamic states. The controls $\tilde{\mathbf{u}}$ may represent actuator inputs, applied forces, throttle position, and relative displacements and rotations of joints.

The requirements for trim can be expressed as follows.

The *trim conditions* are written as

$$\dot{\tilde{\mathbf{u}}} = 0, \quad \forall t, \quad (2)$$

and they state that in trim the controls $\tilde{\mathbf{u}}$ must be constant. The *trim constraints*,

$$\tilde{\mathbf{y}} = \mathbf{y}^*, \quad \forall t, \quad (3)$$

specify the desired values \mathbf{y}^* of the average of some given functions $\tilde{\mathbf{y}}$ of states and controls, here generically called *outputs*. These outputs are defined as follows:

$$\tilde{\mathbf{y}} = \frac{1}{T} \int_{t-T}^t \tilde{\mathbf{g}}(\tilde{\mathbf{x}}, \tilde{\mathbf{u}}) dt, \quad (4)$$

where T is the rotor period.

The particular vehicle prototype and trim problem under study determine the exact physical meaning of the variables $\tilde{\mathbf{y}}$. For free-flight applications, for instance, the outputs can represent the average of global vehicle states which describe its gross motion. In particular, a vehicle-embedded frame can be considered and its linear and angular velocities and orientation parameters with respect to an inertial frame of reference can be taken as outputs. In the simpler case of a rotor connected to the ground (wind tunnel trim), the outputs $\tilde{\mathbf{y}}$ are typically some components of the hub loads expressed in the inertial frame.

Finally, the periodicity of the solution is expressed by the *periodicity conditions*

$$\tilde{\mathbf{x}}(t+T) = \tilde{\mathbf{x}}(t) + \tilde{\mathbf{z}}, \quad \forall t, \quad (5)$$

where $\tilde{\mathbf{z}}$ accounts for possible quasi-periodic states [12].

Model Predictive Auto-pilot

Figure 5 illustrates the non-linear model-predictive auto-pilot proposed in this work. A non-linear reduced model \mathcal{M} of the vehicle is used to predict the (future) response of the plant $\tilde{\mathcal{M}}$, i.e. the rotorcraft comprehensive model, under the action of the control inputs $\tilde{\mathbf{u}}$. Using a reduced model, an optimal control problem is solved on a finite horizon (the *prediction window*). The cost function is chosen to be equal to the norm of the violation of the trim constraints (3), and the optimizer is able to account for possible input and output constraints that may need to be satisfied. In particular, in the present formulation the control actions can vary in time only within the *control window*, while they become constant-in-time from

the end of the control window to the end of the prediction window.

Using the controls computed by the optimizer, the plant is now steered on a short time horizon, the *steering window*, which is here chosen to be equal to the control horizon, although this is not strictly necessary. Once the plant has reached the end of the steering window under the action of the computed control inputs, the optimization problem is solved again, looking ahead in the future over the prediction window shifted forward in time, using a so called *receding horizon* approach. In fact, due to the inevitable mismatch between reduced model and plant, the actual outputs will drift away from the predicted ones, so that optimal control inputs have to be recomputed again.

The reduced model \mathcal{M} is governed by the following system of ordinary differential equations

$$\mathbf{f}(\dot{\mathbf{y}}, \mathbf{y}, \mathbf{u}, \mathbf{p}^*) = 0. \quad (6)$$

The parameters \mathbf{p}^* are assumed to be the result of an adaptation process, which will be discussed later on.

Let $t = T_i^{\text{reg}} = T_i^{\text{steer}}$ be the current time, which is also the beginning of the prediction and steering windows, while $T_f^{\text{reg}} = T_i^{\text{reg}} + \Delta T^{\text{reg}}$ is the end of the prediction window of size ΔT^{reg} . Given initial conditions on the plant states $\tilde{\mathbf{x}}(T_i^{\text{reg}}) = \tilde{\mathbf{x}}_i$, which induce the output initial conditions $\tilde{\mathbf{y}}_i = \tilde{\mathbf{h}}(\tilde{\mathbf{x}})|_{t=T_i^{\text{reg}}}$, the control actions to be applied to the system are computed by solving the following model-predictive regulation problem:

$$\min_{\mathbf{y}, \mathbf{u}} J^{\text{reg}}, \quad (7a)$$

$$\text{s.t. } \mathbf{f}(\dot{\mathbf{y}}, \mathbf{y}, \mathbf{u}, \mathbf{p}^*) = 0, \quad (7b)$$

$$\mathbf{y}(T_i^{\text{reg}}) = \tilde{\mathbf{y}}_i, \quad (7c)$$

$$\mathbf{g}^{\text{reg}}(\mathbf{y}, \mathbf{u}) \in [\mathbf{g}_{\min}^{\text{reg}}, \mathbf{g}_{\max}^{\text{reg}}]. \quad (7d)$$

The regulation cost, J^{reg} , is computed as

$$J^{\text{reg}} = \int_{T_i^{\text{reg}}}^{T_f^{\text{reg}}} M(\mathbf{y}, \mathbf{y}^*, \mathbf{u}) dt, \quad (8)$$

where $M(\mathbf{y}, \mathbf{y}^*, \mathbf{u}) = (\mathbf{y} - \mathbf{y}^*)^T \mathbf{S}_y^{\text{reg}} (\mathbf{y} - \mathbf{y}^*) + \mathbf{u}^T \mathbf{S}_u^{\text{reg}} \mathbf{u} + \dot{\mathbf{u}}^T \mathbf{S}_{\dot{u}}^{\text{reg}} \dot{\mathbf{u}}$, and $\mathbf{S}_y^{\text{reg}}$, $\mathbf{S}_u^{\text{reg}}$ and $\mathbf{S}_{\dot{u}}^{\text{reg}}$

are suitable scaling matrices. The first term in the integral accounts for the regulation error, while the second and third terms are quadratic terms in the control actions and control rates, respectively. The last two terms are typically used for ensuring smooth control policies, through appropriate choices of the weighting matrices.

The solution of the optimization problem satisfies the reduced model governing equations (6) and initial conditions, by means of the constraints (7b) and (7c), and additional possible input and output constraints (7d). In this work, the trim conditions expressed by equation (2) are satisfied in an approximate way by enforcing zero control velocities on the time interval $(T_c^{\text{reg}}, T_f^{\text{reg}})$, i.e.

$$\dot{\mathbf{u}}(t) = 0, \quad T_i^{\text{reg}} < T_c^{\text{reg}} \leq t \leq T_f^{\text{reg}}. \quad (9)$$

Given the periodic nature of the solution of the trim problem, we must have $T_f^{\text{reg}} - T_c^{\text{reg}} > T$, i.e. the constant-in-time condition for the controls must be enforced over a time interval larger than one rotor period. The use of an adaptive element in the reduced model, as described below, allows for the model outputs to match the plant ones with an appropriately small error, and, consequently, for the enforcement of the trim conditions not only at the level of the reduced model but also for the plant, thereby alleviating the appearance of limit cycles in the solution.

The prediction phase is followed by the plant steering phase. Consider the known controls $\mathbf{u}^*(t)$ as obtained by solving problem (7) above, with $t \in \Omega^{\text{steer}} = (T_i^{\text{steer}}, T_f^{\text{steer}})$, where $T_f^{\text{steer}} = T_i^{\text{steer}} + \Delta T^{\text{steer}}$ is the end of the steering window of size ΔT^{steer} . Under the action of the controls \mathbf{u}^* , the plant \mathcal{M} is advanced forward in time starting from the current state $\tilde{\mathbf{x}}_i$. This steering phase amounts to the solution of the following initial value problem:

$$\tilde{\mathbf{f}}(\tilde{\mathbf{x}}, \tilde{\mathbf{x}}, \tilde{\boldsymbol{\lambda}}, \mathbf{u}^*) = 0, \quad (10a)$$

$$\tilde{\mathbf{c}}(\tilde{\mathbf{x}}, \tilde{\mathbf{x}}) = 0, \quad (10b)$$

$$\tilde{\mathbf{x}}(T_i^{\text{steer}}) = \tilde{\mathbf{x}}_i, \quad (10c)$$

which yields a solution in terms of $\tilde{x}(t)$ and $\tilde{\lambda}(t)$ for $t \in \Omega^{\text{steer}}$. The solution at the end of the steering window, $\tilde{x}(T_f^{\text{steer}})$, provides the initial condition for the next regulation and steering phases.

The numerical solution of the model predictive regulation problem (7) can be obtained very efficiently by the direct transcription method [3, 5]. The governing equations of the reduced model are discretized on a computational grid of the regulation window using a numerical scheme, which in this work is the implicit midpoint rule. The discretization defines a set of discrete unknown state and control parameters on the computational grid. Next, the optimization cost function and the constraint conditions are expressed in terms of these discrete parameters. Through this process, the original optimal control problem is transformed into a non-linear programming problem (NLP). The problem is recast in terms of scaled variables, since the numerical solution of optimization problems can be highly sensitive to badly scaled unknowns and constraints.

In this work, the plant steering phase is performed by numerically integrating the multi-body dynamics equations using the nonlinearly unconditionally stable energy decaying scheme described in [1] and references therein. Note that the typical time step size for the plant steering is much smaller than the typical time step size of the model prediction, reflecting the finer solution scales that need to be resolved at the level of the aeroelastic model. Therefore, the controls obtained from the numerical solution of problem (7) have to be properly mapped onto the steering grid, in the present case through a simple interpolation scheme.

The proposed model predictive control approach implies three kind of approximations, related to the mismatch between reduced model and plant, the dimension of the prediction window and the update frequency of the control action.

First, the reduced model is typically able to only approximate the plant dynamics, so the predicted outputs will not be able to exactly render the actual ones. Nevertheless, the

choice of a reasonable reduced model and the adaptation of its parameters allow to control this modeling error.

Second, while in theory large prediction windows (possibly up to T_∞) determine improved stability and a higher performance of the closed-loop system, in practice short horizons are chosen to make the computational cost of the model predictive regulation problem acceptable. In this work a simple finite prediction window is considered. The specialized literature reports several efforts for reducing the effects of this truncation of the prediction horizon (cfr. for example some of the references of [7] and [9]).

Finally, the control actions are updated only after a finite time interval ΔT^{steer} . Since predicted and plant models are different, the outputs of system $\tilde{\mathcal{M}}$ will drift away from the predicted ones under the action of the controls. Clearly, the larger the steering window, the larger this drift will be. On the other hand, short steering windows imply a more frequent solution of the regulation problem. Hence, here again there is a trade-off between these contrasting requirements. In practise, we were always able to determine acceptable activation frequencies of the controller without particular difficulties.

Adaptive Reduced Model

In this work, the reduced model accuracy required to trim a rotorcraft prototype is obtained by recalling well-known system identification techniques. The reduce model \mathcal{M} is parameterized in terms of a discrete number of quantities, indicated by the vector p , and adapted to represent the system behavior as accurately as possible. In other words, the goal of the identification process is to find the set of parameters p^* , and the corresponding reduced model, that produce the best (in some norm) approximation of the plant $\tilde{\mathcal{M}}$ [11]. In particular, \mathcal{M} is here obtained as a reference model augmented by an adaptive neural element, whose role is to approximate the deficiencies of the reference model.

A *reference model* is a specific mathematical model based on insight on the nature of the system (1). This model can be formally expressed as follows:

$$\mathbf{f}_{\text{ref}}(\dot{\mathbf{y}}, \mathbf{y}, \mathbf{u}) = 0, \quad (11)$$

where \mathbf{y} are in this case the states of the reference model subjected to the control inputs \mathbf{u} . The effect of level of detail of the reference model is twofold. On the one hand, it strongly impacts the cost of the numerical solution of the optimal control problem (7), while on the other hand, a more refined reference model is “closer” to the rotorcraft system, in the sense previously discussed.

We note here that the plant controls $\tilde{\mathbf{u}}$ and the reduced model controls \mathbf{u} might represent different physical quantities. In fact the two models describe the system at two different levels of detail, though it is reasonable to assume that it will always be possible to map one set of controls into the other, and viceversa. In the following, without lack of generality, we will assume that the two sets coincide, i.e. $\tilde{\mathbf{u}} = \mathbf{u}$. The reference model (11) is augmented as follows. Let us define the (unknown) function \mathbf{d} as the defect of equations (11) when $\mathbf{u} = \tilde{\mathbf{u}}$ and $\mathbf{y} = \tilde{\mathbf{y}}$, i.e.

$$\mathbf{d}(\tilde{\mathbf{y}}^{(n)}, \dots, \tilde{\mathbf{y}}, \tilde{\mathbf{u}}) = \mathbf{f}_{\text{ref}}(\dot{\tilde{\mathbf{y}}}, \tilde{\mathbf{y}}, \tilde{\mathbf{u}}), \quad (12)$$

where $\tilde{\mathbf{y}}^{(n)}$ indicates the derivative of order n of the outputs with respect to time. If we could correct the reference model by means of \mathbf{d} , the resulting reduced model would ensure the matching of reduced model states and full model outputs ($\mathbf{y} = \tilde{\mathbf{y}}$) when reduced and full models are subjected to the same inputs. However, since this defect function is unknown, we can only identify an approximating operator \mathbf{d}_p belonging to a finite-dimensional class parameterized in \mathbf{p} , so that $\mathbf{d} = \mathbf{d}_p + \varepsilon$, where ε represents the approximation error. Therefore, the resulting reduced model is

$$\mathbf{f}_{\text{ref}}(\dot{\mathbf{y}}_p, \mathbf{y}_p, \mathbf{u}) - \mathbf{d}_p(\mathbf{y}_p^{(n)}, \dots, \mathbf{y}_p, \mathbf{u}, \mathbf{p}^*) = 0, \quad (13)$$

with \mathbf{y}_p being the desired approximation of $\tilde{\mathbf{y}}$. The operator \mathbf{d}_p of equation (13) represents a static non-linear map, so in this work a static

neural network is used for the approximation:

$$\mathbf{d}_p(\dot{\mathbf{y}}, \mathbf{y}, \mathbf{u}, \mathbf{p}) = \mathbf{W}^T \boldsymbol{\sigma}(\mathbf{V}^T \mathbf{x} + \mathbf{a}) + \mathbf{b}, \quad (14)$$

where $\mathbf{x} = (\mathbf{y}^{(n)T}, \mathbf{y}^T, \mathbf{u}^T)^T$ are the network inputs, $\boldsymbol{\sigma}$ a vector of sigmoid activation functions, and $\mathbf{p} = (\dots, W_{ij}, \dots, V_{ij}, \dots, a_i, \dots, b_i, \dots)^T$ the reduced model parameters, i.e. the synaptic weights and biases of the network. A single-hidden-layer feedforward network structure is adopted, where the hidden layer is characterized by N_h neurons connected to the network inputs and outputs by the interconnection weights \mathbf{V} and \mathbf{W} , respectively.

Some aspects are particularly critical for the accuracy of this approximation strategy. First, the network inputs must include as many derivatives of \mathbf{y} as it is necessary to guarantee a sufficiently small error. On the other hand, the universal approximation property of feedforward neural networks [8] ensures that the approximation error can be made arbitrarily small, i.e. it can be bounded as $\|\varepsilon\|_2 \leq C_\varepsilon$ for any $C_\varepsilon > 0$, for some appropriately large number of hidden neurons N_h . However, this result only guarantees the existence of an optimal set of parameters \mathbf{p} . Several methods are available to tune the reduced model and minimize the approximation error [6]. In this research, the parameters \mathbf{p} are held equal to $\mathbf{p}(T_f^{\text{steer}})$ during the steering phase. Then, the local information provided by the plant response is used to adapt the network and correct the parameters. In particular, if $\tilde{\mathbf{y}}_f^* = \tilde{\mathbf{y}}^*(T_f^{\text{steer}})$ and $\mathbf{u}_f^* = \mathbf{u}^*(T_f^{\text{steer}})$ are respectively the plant outputs and given control inputs at the end of the steering window, we measure the mismatch

$$E = \left\| \mathbf{f}_{\text{ref}}(\tilde{\mathbf{y}}_f^*, \tilde{\mathbf{y}}_f^*, \mathbf{u}_f^*) - \mathbf{d}_p(\tilde{\mathbf{y}}_f^{*(n)}, \tilde{\mathbf{y}}_f^*, \mathbf{u}_f^*, \mathbf{p}) \right\|_2, \quad (15)$$

which is a function of the parameters \mathbf{p} . The updated value of the parameters, $\mathbf{p}(T_f^{\text{steer}})$, is obtained by using the steepest-descent search direction as

$$\mathbf{p}(T_f^{\text{steer}}) = \mathbf{p}(T_i^{\text{steer}}) - \eta \frac{\partial E}{\partial \mathbf{p}} \Big|_{\mathbf{p}(T_i^{\text{steer}})}, \quad (16)$$

where η is the so called “learning rate”. The updated parameters can then be used for the next prediction and steering phases.

Numerical Results

In this section, a multibody model of the rotor of the UH-60 helicopter is used to compare the behavior of the proposed NMP auto-pilot and an available implementation of the classical auto-pilot approach. This four-bladed articulated rotor model is characterized by the typical flap-lag-pitch configuration (from the hub to the blade), with three coincident hinges which are offset from the rotor shaft axis. The blades are modeled as geometrically exact beams, and are meshed using 6 cubic finite elements along the span. In the rotor model, the rotation of the pitch hinge θ_i of the i th blade is driven according to the following expression: $\theta_i(\psi) = \theta_0 + \theta_{1s} \sin(\psi - i\pi/2) + \theta_{1c} \cos(\psi - i\pi/2)$, $i = 1, 2, 3, 4$, where ψ is the azimuthal angle of the rotor, θ_0 is the rotor collective, θ_{1s} is the longitudinal cyclic and θ_{1c} the lateral one.

The aerodynamic characteristics of the rotor are modeled through the use of lifting lines based on sectional aerodynamic coefficients, stored in look up tables, and using 30 airstations on each blade. Higher accuracy of the model could be achieved by using proper aerodynamic modules to render the rotor wake effect. However, here we will simply use strip theory to represent the rotor aerodynamics. Despite this lack of accuracy, we can consider this multibody model a good test-bed for the proposed auto-pilot, because of the presence of flexible elements with complex geometric, inertial and aerodynamic properties.

We consider the wind-tunnel trim of the rotor for different values of the advance ratio μ . At first, estimates are obtained for the target hub forces required to trim the helicopter at each value of μ . The estimated target loads are computed by using simple power balance relations and basic information on the vehicle, like take-off weight, distance between main and tail rotor, solidity of the main rotor, etc. [10]. Then, for each given value of the advance ratio, the multibody model is steered to the corresponding target values. Seven simulations are performed for each controller, between $\mu = 0$ and 0.35. At the beginning of each simulation, the collective, longitudinal and lateral cyclics are

set to 4, 0 and 0 deg, respectively, and the rotor response follows the periodic orbit obtained in correspondence to these values of the control settings, by simulating the system forward in time until all transients decay. Then, the chosen controller is activated.

According to [12], a possible discrete-time proportional auto-pilot control law is

$$\tilde{\mathbf{u}}_f = \tilde{\mathbf{u}}_i + \Delta t \mathbf{S}^{-1} \mathbf{G} (\mathbf{y}^* - \tilde{\mathbf{y}}), \quad (17)$$

where $\tilde{\mathbf{u}}_i$ and $\tilde{\mathbf{u}}_f$ are respectively the controls at the beginning and at the end of a time step, and $\mathbf{y}^* - \tilde{\mathbf{y}}$ is the error on the trim constraints (3). The matrix \mathbf{G} , in general taken as $\mathbf{G} = \text{diag}(\mathbf{g}_0)$, represents a set of gains, which must be properly tuned in order to obtain a stable solution and an acceptable performance. Finally, \mathbf{S} indicates the sensitivity matrix of the outputs with respect to the inputs, namely $\mathbf{S} = \partial \tilde{\mathbf{y}} / \partial \mathbf{u}$. Preliminary tests allowed to tune the classical auto-pilot gains \mathbf{g}_0 . In the following, we will refer to two different situations: *classical auto-pilot A*, tuned by trimming the rotor with maximum performance (shortest time) at $\mu \approx 0.2$, and *classical auto-pilot B*, optimized for $\mu \approx 0.25$.

The NMP auto-pilot has an activation frequency equal to 4/rev, a prediction horizon of 3 revolutions and control rates limited to 10 deg/sec. The neural network has 20 neurons in its hidden layer, and was adaptively trained starting from small random values throughout each maneuver with a learning rate set to 0.3. Clearly, even faster convergence to the solution with respect to what shown below could have been obtained by using as starting guesses for the network parameters those computed at the previous value of the advance ratio. This further exploitation of the adaptive nature of the controller was however avoided here to give a more conservative estimate of its performance.

In order to quantify the ability of the auto-pilots to trim the system, a criterion is required to indicate when the trim solution is achieved within a desired tolerance. To this purpose, we define the *time to trim* as

$$T_{\text{trim}} : \varepsilon_{\text{con}}(t) \leq \varepsilon_{\text{con}}^{\text{max}}, \forall t \geq T_{\text{trim}}, \quad (18)$$

where $\varepsilon_{\text{con}}(t) = \|\tilde{\mathbf{y}}_s(t) - \mathbf{y}_s^*\|_2$ is the norm of the error on the trim constraints (3) at each instant of time. The quantity $\varepsilon_{\text{con}}^{\text{max}}$ is the user-specified maximum allowed error on the trim constraints, a parameter that strongly affects the value of the time to trim.

Table 1: Revolutions needed to trim the rotor model according to definition (18) for different advance ratios μ and auto-pilots, and with $\varepsilon_{\text{con}}^{\text{max}} = 0.05$ (top) and $\varepsilon_{\text{con}}^{\text{max}} = 0.01$ (bottom). \times : convergence not achieved.

| μ | Classical auto-pilot A | Classical auto-pilot B | NMP auto-pilot |
|-------|------------------------|------------------------|----------------|
| 0.00 | 11.6 | 38.5 | 1.8 |
| 0.05 | 9.2 | 32.3 | 2.9 |
| 0.10 | 6.2 | 22.1 | 4.4 |
| 0.15 | 5.4 | 13.4 | 5.2 |
| 0.20 | 5.5 | 9.9 | 5.8 |
| 0.25 | 14.6 | 11.8 | 6.6 |
| 0.30 | \times | \times | 9.0 |
| 0.35 | \times | \times | 11.6 |

| μ | Classical auto-pilot A | Classical auto-pilot B | NMP auto-pilot |
|-------|------------------------|------------------------|----------------|
| 0.00 | 18.1 | 60.4 | 4.6 |
| 0.05 | 15.7 | 52.3 | 6.5 |
| 0.10 | 11.6 | 38.4 | 6.5 |
| 0.15 | 8.2 | 26.0 | 8.1 |
| 0.20 | 8.2 | 17.4 | 8.7 |
| 0.25 | 28.1 | 18.2 | 9.6 |
| 0.30 | \times | \times | 14.4 |
| 0.35 | \times | \times | 19.6 |

In Table 1 we report the time to trim for varying μ . The upper table summarizes the results for $\varepsilon_{\text{con}}^{\text{max}} = 0.05$, while the lower one for $\varepsilon_{\text{con}}^{\text{max}} = 0.01$. The results show that the classical auto-pilots perform nicely when they are operating close to the values of μ for which they were calibrated, and their trim time is of the same order of magnitude as the NMP auto-pilot. However, for $\mu > 0.25$ both controllers A and B failed to find a trimmed solution, either because the feedback control system went unstable or because the solution resulted in a limit cycle; hence, the cross symbols in the table indicate values of the advance ratio that are outside of the operational limits of the classical auto-

pilots. Not only the classical approach is not always able to trim the system, but sometimes it does so only at unacceptable trim times. More reasonable trim times at low advance ratios can be obtained by optimizing (increasing) the gains in the neighborhood of those values. This however can shrink even more the auto-pilot operational region. Therefore, a suitable gain scheduling strategy is needed to guarantee stability and reasonable performance on a wide range of flight conditions.

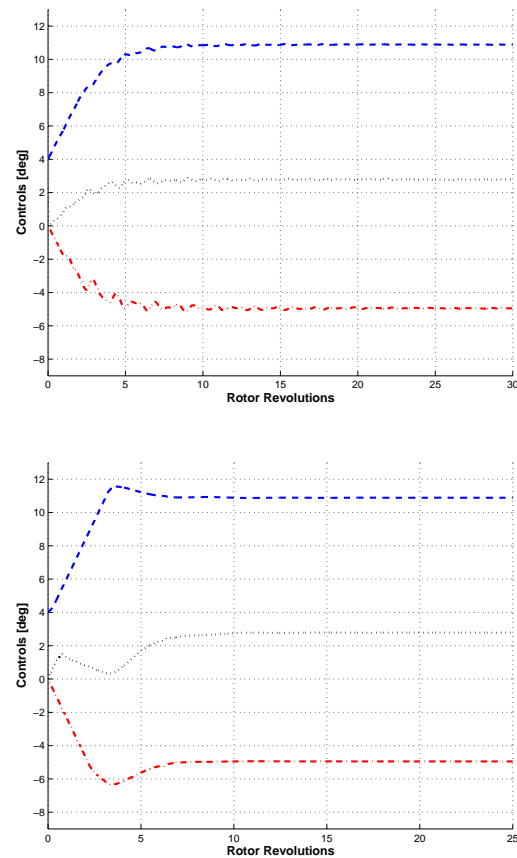


Figure 1: Control time history for the classical auto-pilot A (top), and the NMP auto-pilot (bottom), $\mu = 0.25$.

Table 1 reports also a completely different behavior of the predictive auto-pilot: the time to trim slightly increases with the advance ratio, evidence that the procedure is robust with re-

spect to the flight condition. Furthermore, the controller was able to successfully reach the desired trim condition up the highest value of μ .

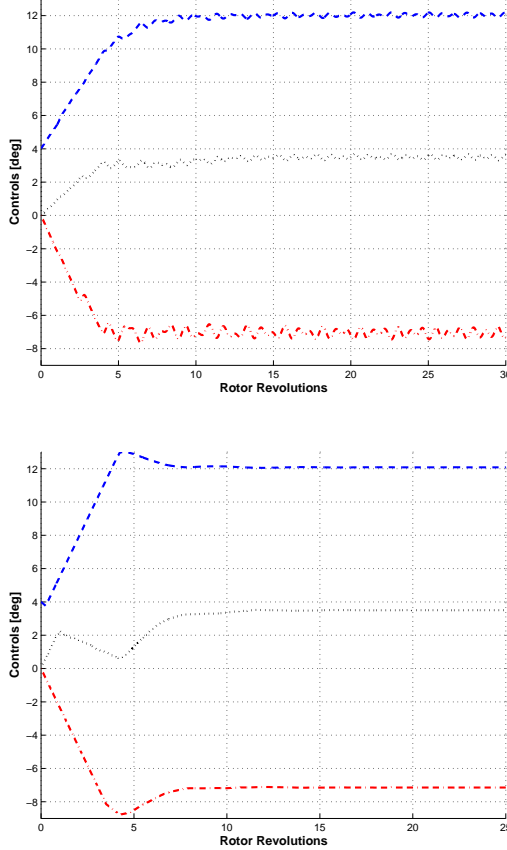


Figure 2: Control time history for the classical auto-pilot A (top), and the NMP auto-pilot (bottom), $\mu = 0.297$.

Figures 1-4 give a even clearer idea of the situation: for $\mu = 0.25$ (Figures 1) the classical and predictive controllers show a very similar behavior, and they converge quickly to the trimmed solution.

The increase of μ up to the value 0.297 (Figures 2) seems not to influence the NMP auto-pilot. On the contrary, the proportional controller finds a solution characterized by oscillating control time histories. This result seems coherent with the absence of direct knowledge

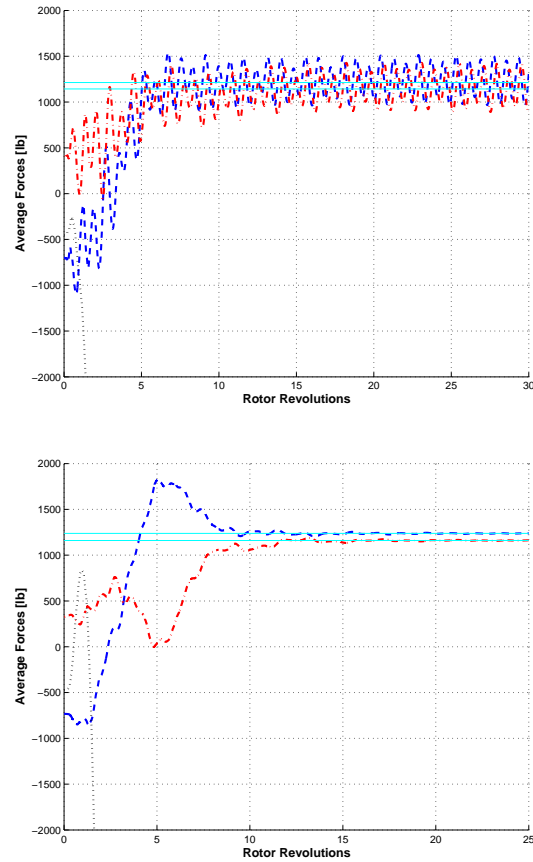


Figure 3: Output time history for the classical auto-pilot A (top), and the NMP auto-pilot (bottom), $\mu = 0.297$. Solid lines: target values.

of the trim conditions (2) in the classical auto-pilot approach. Figure 3 shows the time histories of the corresponding rotor loads, where the horizontal solid lines now indicate the desired target values. For this figure, the plot range is such that the third component of the rotor force is left out of the plot; this shows more clearly the behavior of the two smaller components. The NMP controller achieves constant-in-time values of the control inputs and of the average-over-the-period rotor loads, as required by a trimmed condition.

Finally, Figure 4 shows, for $\mu = 0.3$, the predictive controller converging to the trim solution, similarly to the previous tests, and the unsta-

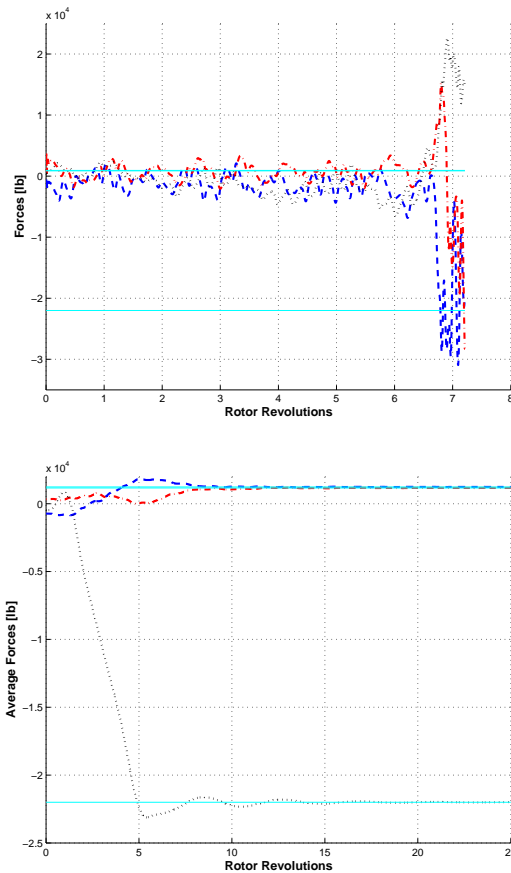


Figure 4: Hub load time history for the classical auto-pilot A (top), and output (i.e. hub load average over the rotor period) time history for the NMP auto-pilot (bottom), $\mu = 0.3$. Solid lines: target values.

ble response of the hub loads for the classical auto-pilot, which is not able to trim the rotor at this speed.

Conclusions

A new auto-pilot technique to trim virtual models of rotorcraft has been proposed, with the aim of removing some of the deficiencies of current auto-pilots, while still maintaining their basic positive feature, i.e. the applicability to arbitrarily complex virtual models of the vehi-

cle. The methodology is based on a neural-adaptive non-linear model predictive controller, and it was tested and compared with a classical auto-pilot formulation based on a suitable set of gains. In the reported numerical experiments, the non-linear reduced model used to predict the system response seems to imply superior performance of the controller with respect to conventional approaches, similarly to other examples in the literature for difficult, highly non-linear control problems. Moreover, the proposed auto-pilot specifically accounts for the presence of the constant-in-time constraints on the control actions in the prediction problem. The effect of constraints is difficult to incorporate in other control strategies, which often show limit-cycle oscillations of the inputs. Theoretical arguments ensure the absence of such limit cycles for the presented predictive approach provided that the reduced model perfectly matches the plant and for an infinite prediction window. Although these conditions are not satisfied in practice, no limit cycles were observed using the described implementation.

Another characterizing feature of the proposed auto-pilot is its adaptive nature. Adaptivity allows for the reduced model to learn the behavior of the plant and guarantees the convergence of the aeroelastic system to the desired trim solution. This control strategy should be easily extendable to virtually any rotorcraft mathematical model, possibly including complex aerodynamic effects, without *ad hoc* modifications or tuning.

References

- [1] Bauchau, O.A., Bottasso, C.L., and Trainelli, L., "Robust Integration Schemes for Flexible Multibody Systems", *Computer Methods in Applied Mechanics and Engineering*, Vol. 192, 2003, pp. 395–420.
- [2] Bauchau, O.A., Bottasso, C.L., and Nikishkov, Y.G., "Modeling Rotorcraft Dynamics with Finite Element Multibody

- Procedures”, *Mathematics and Computer Modeling*, Vol. 33, 2001, pp. 1113–1137.
- [3] Betts, J.T., *Practical Methods for Optimal Control Using Non-Linear Programming*, SIAM, Philadelphia, PA, 2001.
- [4] Bhagwat, M.J., and Leishman, J.G., “Stability, Consistency and Convergence of Time Marching Free-Vortex Rotor Wake Algorithms”, *Journal of the American Helicopter Society*, Vol. 46, 2001, pp. 59–71.
- [5] Bottasso, C.L., Chang, C.-S., Croce, A., Leonello, D., and Riviello, L., “Adaptive Planning and Tracking of Trajectories for the Simulation of Maneuvers with Multibody Models”, *Computer Methods in Applied Mechanics and Engineering*, accepted, to appear in the special issue “Computational Multibody Dynamics”.
- [6] Fausett, L., *Fundamentals of neural networks*, Prentice Hall, New York, NY, 1994.
- [7] Findeisen, R., Imland, L., Allgöwer, F., and Foss, B.A., “State and Output Feedback Nonlinear Model Predictive Control: An Overview”, *European Journal of Control*, Vol. 9, 2003, pp. 190–207.
- [8] Hornik, K., Stinchcombe, M., and White, H., “Multi-Layer Feed-Forward Networks Are Universal Approximators”, *Neural Networks*, Vol. 2, 1989, pp. 359–366.
- [9] Jadbabaie, A., Yu, J., and Hauser, J., “Unconstrained Receding-Horizon Control of Nonlinear Systems”, *IEEE Transactions on Automatic Control*, Vol. 46, 2001, pp. 776–783.
- [10] Leishman, G., *Principles of Helicopter Aerodynamics*, Cambridge University Press, Cambridge, MA, 2000.
- [11] Narendra, K.S., and Parthasarathy, K., “Identification and Control of Dynamical Systems Using Neural Networks”, *IEEE Transactions on Neural Networks*, Vol. 1, 1990, pp. 4–27.
- [12] Peters, D.A., and Barwey, D., “A General Theory of Rotorcraft Trim”, *Mathematical Problems in Engineering*, Vol. 2, 1996, pp. 1–34.
- [13] Peters, D.A., and He, C.J., “Finite State Induced Flow Models. Part II: Three-Dimensional Rotor Disk”, *Journal of Aircraft*, Vol. 32, 1995, pp. 323–333.
- [14] Rutkowski, M., Ruzicka, G.C., Ormiston, R.A., Saberi, H., and Jung, Y., “Comprehensive Aeromechanics Analysis of Complex Rotorcraft Using 2GCHAS”, *Journal of the American Helicopter Society*, Vol. 40, 1995, pp. 3–17.

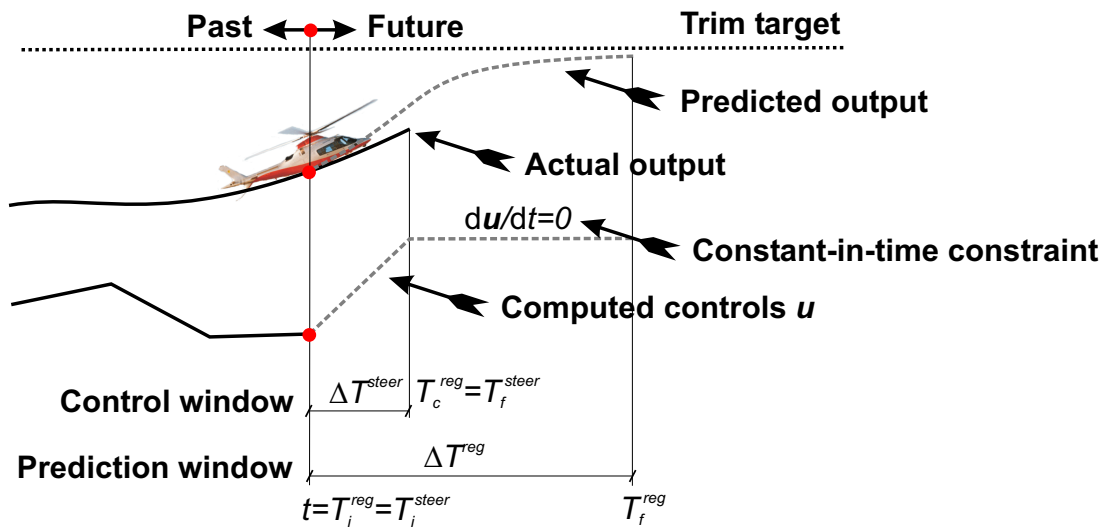


Figure 5: Schematic illustration of the model-predictive auto-pilot method, with the indication of the different time windows.